Evaluation of the Shutdown Time of Subsea Pipeline for Oil Transportation

D. Maciel[1], N. Bouchonneau*[1]

[1]Universidade Federal de Pernambuco, Recife, Pernambuco, Brazil
*nadege.bouchonneau@gmail.com

Abstract: The maintenance plan or rush-to-repair of a subsea pipeline for oil transport may result in the shutdown of the line, in other words, may stop the flow of fluid. During the shutdown, the temperature of the oil tends to decrease continuously, and the heavy molecules tend to crystallize and suspend in the oil, which increase the viscosity of the oil, and even form a paraffinic compound or freeze the production line.

This work was carried out in order to analyze the temperature distribution in an insulated pipeline during its restart (transient state), work (steady state) and shutdown, and estimate the time required to reach the critical temperatures of approximately 40 and 25 ºC during the shutdown. Moreover, with the results assist the procedures of maintenance and restart, and ensure that they are safe, effective and economical.

Keywords: pipeline, thermal insulation, oil transport, shutdown, finite element method.

1. Introduction

Once the line is frozen during the shutdown, it is necessary to use complex time-consuming procedures and expensive methods to unlock it and restart the production. Therefore, it is important to conduct experimental and computational studies to analyze and better understand the behavior of lines submitted to a shutdown of the production and the evaluation of the time required to reach critical freezing temperatures (shutdown time), in order to present a safe, effective and economic proposal for the restart of the production.

In order to study the behavior of insulated structures, simulations based on the Finite Element Method (FEM) were performed with COMSOL Multiphysics software to compare numerical results with those obtained experimentally in the literature. One expects to find values consistent with the actual obtained in the subsea oil industry, and characterize insulated pipelines in service conditions.

Therefore, the main objective of this work is to develop and validate a suitable numerical model, which can predict the thermomechanical behavior of pipes with multilayer insulation subjected to conditions of ultra-deep service, and thus determine the critical time of shutdown according to the operation field.

2. Experiment

2.1. Insulated pipe structure

The industrial structure (1.2 m initial length) consists of a steel pipe (internal diameter of about 180 mm, thickness about 18 mm) and a 5-layer insulating coating (total thickness 61mm) which were industrially applied by side extrusion process, detailed by Berti (2004). The coating is composed of several material types: solid, adhesive polymers and syntactic foam, which is composed of hollow glass microspheres embedded in a polypropylene matrix. One advantage to combine varied materials is the possibility to obtain mechanical and thermal properties as well as good long-term behavior in water required for deep-sea application, all these properties being difficult to obtain with a single material. The multilayered system and the material thicknesses are presented in Fig. 1, taken from Bouchonneau *et al.* (2010).

Material	Thickness (mm)
Steel pipe	18,26
Epoxy powder primer	0,25
Adhesive PP	0,25
Solid PP	3
Syntactic PP	55
Solid PP	2,5

Table 1. Composition of the insulated pipe.

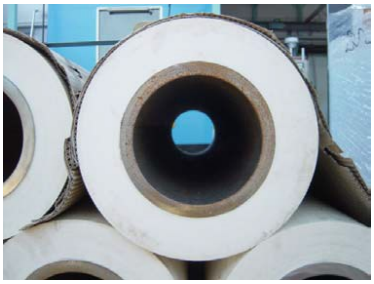

Figure 1. Industrial 5-layer insulation system.

2.2. Material properties

Thermal and mechanical properties of each constitutive material of the test section are reported, respectively, in Tables 2 and 3, adapted from Bouchonneau *et al.* (2010).

Material	Thermal conductivity (W/m.K)	Heat Capacity (J/kg.K)
Steel pipe	45	475
Fusion bonded epoxy	0,3	2000
Adhesive PP	0,22	2090
Solid PP	0,22	2000
Syntactic PP	$0{,}165+10^{-4}.T$	1506,6+6,26.T
Steel cap – APX4	19	460
PTFE (insulating end cap)	0,24	1050

Table 2. Thermal properties.

The values given for the PP syntactic foam were collected from experimental measurements performed at 1 bar on small samples. In addition, for the steel pipe and the polymers, values from the literature were used as input data in the simulation.

Material	Density (kg/m^3)	Elastic modulus (GPa)	Poisson coefficient	Expansion coefficient ($°C^{-1}$)
Steel pipe	7850	218	0,33	1.10^{-5}
Epoxy	1200	3	0,4	$5{,}3.10^{-5}$
Adhesive PP	900	1,3	0,4	$1{,}6.10^{-4}$
Solid PP	900	1,3	0,4	$1{,}6.10^{-4}$
Syntactic PP	640	$1{,}1\text{-}0{,}94.10^{-3}.T$	0,32	5.10^{-5}
Steel cap	7700	211	0,33	1.10^{-5}
PTFE	2200	0,4	0,46	$1{,}3.10^{-4}$

Table 3. Mechanical properties.

2.3. In service tests

Experimental tests on the industrial prototype contribute to develop and complete a multiscale approach by collecting experimental data on an entire structure tested under representative service conditions of pressure and temperature. The tests also contribute to discuss the validity of the numerical modelling.

2.4. Testing facilities

For the prototype testing, a high pressure vessel (1 m diameter, 2 m height, up to 1000 bar) located in IFREMER Brest was used.

The pressure inside the vessel is regulated and monitored using a pressure transducer mounted at the top of the pressure vessel. The water temperature inside the pressure tank (about 15 °C in this study) is also regulated and monitored during the tests. A schematic view of the coated test pipe in vertical position during testing in the pressure vessel is given in Fig. 2, taken from Bouchonneau *et al.* (2010). The number of sensors for the prototype instrumentation was limited by the number of connections available on the pressure vessel flange.

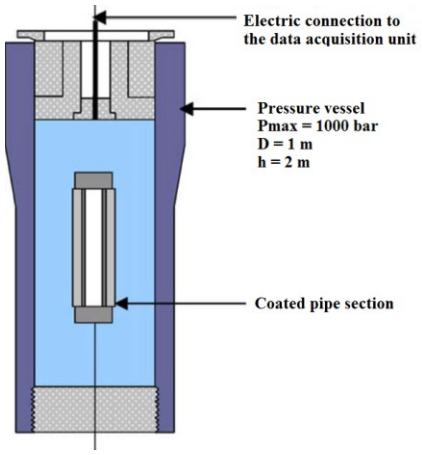

Figure 2. Schematic representation of the insulated pipe section during hyperbaric tests.

2.5. Equipment

The insulated pipe section was machined at both ends to adapt two metallic steel caps in Stainless steel (APX4) covered by 100 mm thick Polytetrafluoroethylene (PTFE) insulating caps in order to limit axial heat flowlosses. The metallic caps were also equipped with connectors resistant to high external pressure. Three 10-channel connectors were necessary to allow the electrical supply of the inner heating system (one connector) and to collect inner sensor data (two connectors). The different elements that equipped the prototype are shown on Fig. 3, taken from Bouchonneau *et al.* (2010).

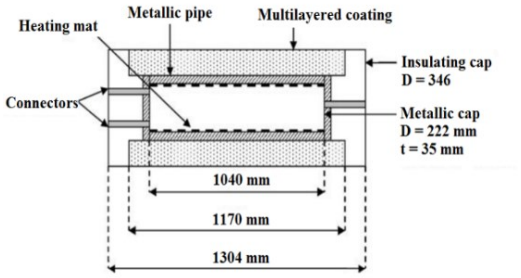

Figure 3. Prototype equipment.

2.6. Instrumentation

The schematic representation of the fully instrumented pipe section and the location of sensors are given in Fig. 4, taken from Bouchonneau *et al.* (2010). The insulated pipe section was instrumented with six commercial temperature sensors (Pt100) specified up to 200 °C minimum (accuracy of about 0.3% at 100 °C), located in both inner and outer parts along the pipe length and on the caps (Fig. 4):

- T_i (°C): inner temperature of the steel surface in the center of the pipe (one measurement);
- T_e (°C): outer temperature of the coating surface in the center of the pipe (one measurement);
- T_b (°C): inner temperature of the steel surface in the center of one cap (one measurement);
- T_{100} (°C): inner temperature of the steel surface along the pipe 100 mm distant from cap (one measurement);
- T_{50} (°C): inner temperature of the steel surface along the pipe 50 mm distant from cap (one measurement).

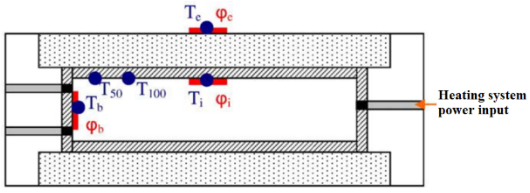

Figure 4. Instrumentation of the industrial prototype.

Besides, the outer temperature of the water in the vessel, T_{water} (°C), was also measured using a platinium sensor.

The insulated pipe section was also instrumented with four commercial heat flux sensors located in both inner and outer parts along the pipe length and the caps:

- φ_i (W m^{-2}): inner thermal flux density on the steel surface in the center of the pipe (one measurement with soft circular fluxmeter of 5 µV m^2 W^{-1} sensitivity specified up to 200 °C);
- φ_e (W m^{-2}): outer thermal flux density on the coating surface in the center of the pipe (three measurements with a semi-rigid fluxmeter of 50 µV m^2 W^{-1}) sensitivity specified up to 100 °C and 100 bar (one measurement with a rigid fluxmeter of 30 µV m^2 W^{-1} sensitivity specified up to 250 °C and 150 bar);
- φ_b (W m^{-2}): inner thermal flux density on the steel surface in the center of the steel cap (one measurement with rigid rectangular fluxmeter of 36 µV m^2 W^{-1} sensitivity specified up to 200 °C).

Heat flux sensors with soft flat form were selected for the internal and external pipe surfaces to reduce errors related to the difficulties in mounting rigid flat sensors.

The readings obtained from all the sensors were recorded by a data acquisition unit, which could be programmed to take recordings at appropriate time intervals throughout the duration of the test.

2.7. Testing procedures

For the experimental testing, a prototype structure has been instrumented and tested successively without additional pressure (external pressure of 1 bar — test A) and under 300 bar hydrostatic pressure (test B), simulating in-service conditions at about 3000 m depth, at two different conditions of inner temperature, in order to study the influence of pressure and temperature on the thermal performances of the structure. Both test sequence programs are shown in Fig. 5, taken from Bouchonneau *et al.* (2010).

The test sequences have been chosen in order to be representative of service conditions (pressure then temperature). In both cases, it should be emphasized that a test lasting approximately 10 days cannot be used to predict the long term evolution of the insulation coating systems for which water uptake and creep cannot be neglected.

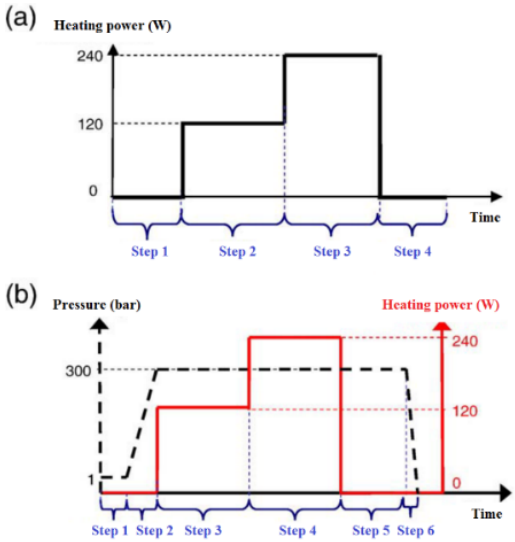

Figure 5. Testing programs realized on the prototype.

3. Use of COMSOL Multiphysics

The computational geometry, finite element mesh and boundary conditions of the improved model used to study the thermal insulation pipe multiple layers are presented in Fig. 6. This model follows the conditions described by Bouchonneau *et al.* (2010), which are based on following hypotheses: internal convection between the air and the inner surface of the prototype, external convection between the water and the pipeline, hydrostatic pressure of the water on external surfaces of the prototype, and internal heat flux. Besides, the model consider the presence of the connector to link the experimental sensors, located at the center of the PTFE cap and is responsible for much of the longitudinal heat loss.

Depending on the test and step, different experimental conditions (temperature, pressure, etc.) are applied to the structure. Therefore, the boundary and initial conditions of the model vary depending on each experimental step, and the input data used for the model are described in Tables 4 and 5. Furthermore, the initial temperatures of 240 W models are evaluated from the result of the steady state in 120 W models.

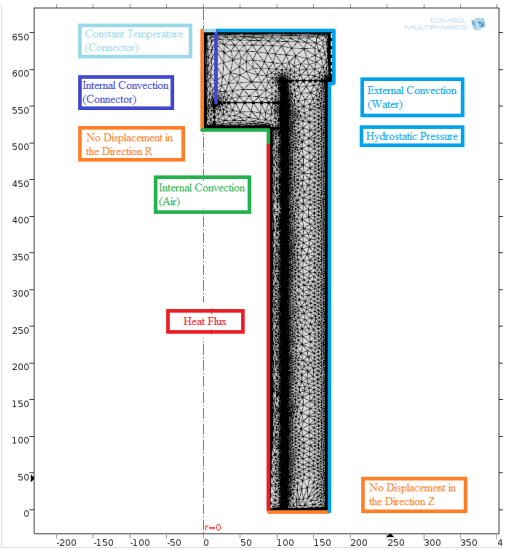

Figure 6. Geometry, mesh and boundary conditions of the improved model.

Experimental Step	Pressure (bar)	Heat Flux (W/m²)	Initial Temp. (°C)	Water Temp. (°C)	Coefficient of External Convection – h_e (W/m².K)
Test A/ Step 2	1	210	15,36	15,25	125
Test A/ Step 3	1	420	-	15,3	155
Test B/ Step 3	300	210	16,62	16,75	170
Test B/ Step 4	300	420	-	17,27	230

Table 4. Boundary conditions.

Experimental Step	Air Temp. (°C)	Coefficient of Internal Convection - h_i (W/m².K)	Constant Temp. in the end of Connector (°C)	Coefficient of Internal Convection in the Connector – h_{i2} (W/m².K)
Test A/ Step 2	30	3	15,25	0,29
Test A/ Step 3	60	3,7	15,3	0,29
Test B/ Step 3	30	3	16,75	17,6
Test B/ Step 4	60	3,7	17,27	96,7

Table 5. Complementary boundary conditions described by Bouchonneau *et al.* (2010).

4. Results

4.1. Results from the steady state of the improved model

First, the stationary or operation state of the pipeline with multilayer insulation was simulated, resulting in multiple charts for each test step. Here, Fig. 7 shows the most important results, from the case of 300 bar and 240 W, the distributions of temperature, displacement, stress,

resulting from the simulations for the case of 300 bar and 240 W.

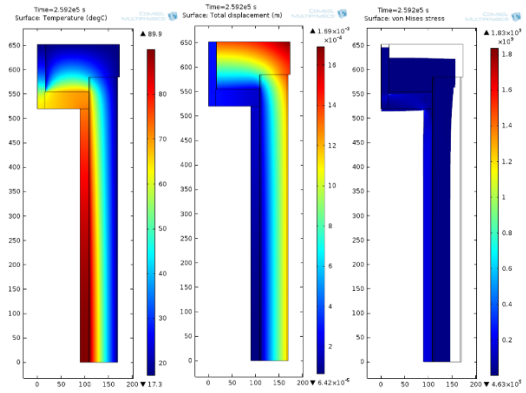

Figure 7. Results of the steady state of the improved model (deformed scale 200:1), in the case of 300 bar e 240 W.

The results of the temperature distribution in all stages of testing, shows a temperature gradient in the longitudinal direction, which indicates that there is a significant heat loss in that direction. This loss of heat is obtained mainly due to the metal cap and the connector, which have high thermal conductivity, allowing heat to pass more easily.

4.2. Results from the transient state of the improved model and comparison with the experimental

Then, comparisons between the simulated and experimental temperatures of the prototype were made during the transient regime, based on the location of the temperature sensors used in the tests. These are presented in Graphs 1 and 2, resulting from the simulations for the case of 300 bar (Test B).

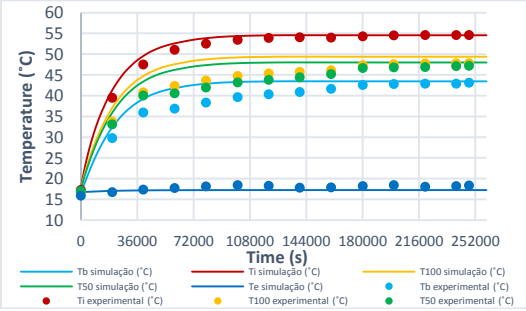

Graph 1. Comparison between experimental and simulated temperatures, during the test at 300 bar and 120 W.

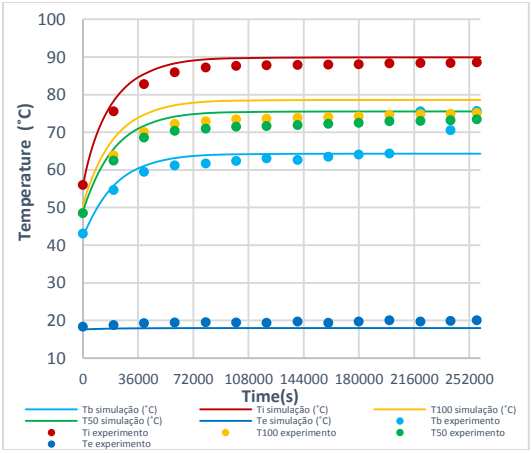

Graph 2. Comparison between experimental and simulated temperatures, during the test at 300 bar and 240 W.

The numerical results obtained for the improved model showed good agreement with experimental values, particularly regarding to T_i and T_b temperatures. Therefore, it allows to validate the thermomechanical modeling proposed in this work and the stationary state obtained in both structures. Then, shutdown simulations were performed in order to evaluate the behavior of the structure during cooling, and the hypothesis and results will be presented in paragraph 4.4.

4.3. Analysis of the heat flow loss in the connector and PTFE cap

With the completion of the analysis of the improved model, it appeared interesting to evaluate the heat losses flowing through the connector and the PTFE cap. To perform this evaluation, it was necessary to integrate in line and then in surface the heat flow along the desired region of the improved model, with the help of COMSOL Multiphysics tools (see Figs. 8 and 9).

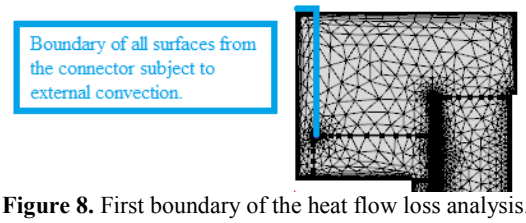

Figure 8. First boundary of the heat flow loss analysis.

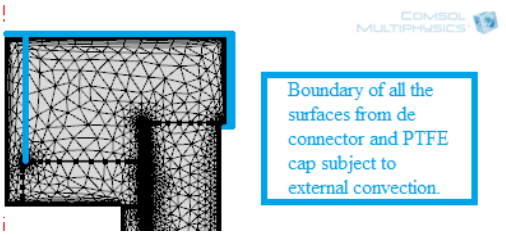

Figure 9. Second boundary of the heat flow loss analysis.

The results of the improved model for the case of 240 W and 300 bar, presented in the Graphs 3 and 4, show that the heat losses flowing through the connector reach 10.94 W, or about 4.56% of the power supplied for heating the prototype. Moreover, considering the symmetry of the model, the heat flow losses across the prototype through connectors is actually double, 20.88 W representing about 9.12% of heating power.

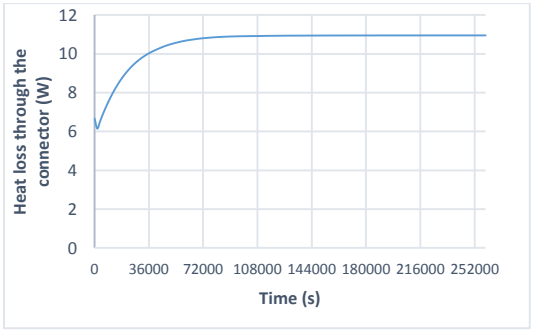

Graph 3. Result of the heat flow loss across connector in the case of 240 W and 300 bar.

The heat flow loss across the connector and PTFE cap reaches 20.53 W, or 8.55% of the heating power of the prototype. Thus, heat lost by the connector is about 53.30%, longitudinal heat loss being even more relevant in this model.

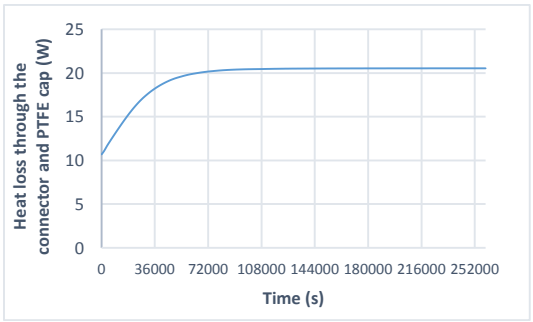

Graph 4. Result of the heat flow loss across connector and PTFE cap in the case of 240 W and 300 bar.

4.4. Evaluation of the critical shutdown time

Based on the results obtained at stationary state, further simulations were performed to evaluate the behavior of the structure during a shutdown, i.e. when the internal heat flow is suddenly turned to zero. For this study, in order to evaluate the critical time of shutdown of the insulated pipe, simulations were performed to models after completion of test B/step 4 (240 W, 300 bar). Simulations with no internal heating power were then performed so that cooling of the pipeline can be analyzed in case of an emergency stop or maintenance. The results of simulated shutdown are presented in Graph 5. These curves enable to estimate the critical time to reach the shutdown temperature of 40 ºC, when the intensification of formation of paraffinic compounds occurs in the line, and at a temperature of 25 ºC, when freezing of the line occurs.

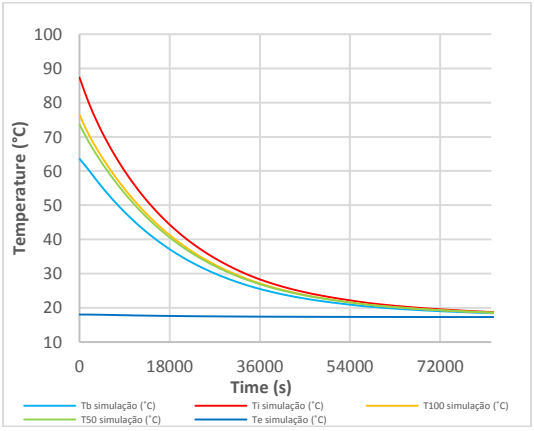

Graph 5. Results of the shutdown of the improved model, in the case of 300 bar e 240 W.

By analyzing the results presented in Graph 5, the critical time to reach shutdown temperatures of 40 °C can be evaluated to 21532.7 s or 5 h 58 min. The critical time to reach shutdown temperatures of 25 °C, corresponding to the beginning of freezing of the line is 43769.9 s or 12 h 09 min. It should be emphasized that all these values were obtained by linear interpolation of the results.

6. Conclusions

In this work, a thermomechanical model of an instrumented pipe has been proposed to better

represent instrumentation and experimental conditions applied to the structure. The simulation results obtained for inner and outer temperatures show good agreement with experimental data. Based on the numerical results, it was also possible to highlight relevant axial heat losses through the end caps and metallic connector. After validating the modeling, numerical simulations were performed based on the same model to simulate shutdown conditions. Based on numerical results, it could be concluded that after about 6 h of shutdown occurring in such a line of subsea oil transport, intensification will occur in the formation of paraffinic compounds, which could complicate the process of restarting the line. After about 12 h, beginning of freezing will occur in the line, preventing traditional methods of restart, based on the injection of high-pressure fluid. Therefore, such arrangements should be made in the maintenance plans and restarting of subsea lines, to ensure that the procedure taken is safe, effective and economical. COMSOL show to be a great tool to obtain rapidly estimations of critical shutdown times in pipelines, which could thus help to make quickly safe decisions about maintenance and restarting procedures.

7. References

1. BERTI, E., 2004. Syntactic polypropylene coating solution provides thermal insulation for Bonga risers, Offshore Magazine, 64, 2. http://www.offshoremag.com/currentissue/index.cfm?p=9&v=64&i=2.

2. BOUCHONNEAU, N., SAUVANT-MOYNOT, V., CHOQUEUSE, D., GROSJEAN, F., PONCET, E., PERREUX, D., 2007. Thermal insulation material for subsea pipelines: benefits of instrumented full scale testing to predict the long term thermo-mechanical behaviour. Proceedings of the Offshore Technology Conference — OTC 18679, Houston, Texas, USA.

3. BOUCHONNEAU, N., SAUVANT-MOYNOT, V., CHOQUEUSE, D., GROSJEAN, F., PONCET, E., PERREUX, D. Experimental testing and modelling of an industrial insulated pipeline for deep sea application. Journal of Petroleum Science and Engineering 73, p. 1–12 (2010).

4. COMSOL, COMSOL Multiphysics, Multiphysics Modeling Guide (2008).

5. LEFEBVRE, K., SAUVANT-MOYNOT, V., CHOQUEUSE, D., CHAUCHOT, P., 2006. Durabilite des materiaux syntactiques d'isolation thermique et de flottabilite: des mecanismes de degradation a la modelisation des proprietes long terme. Proceedings of the Conference: Materiaux 2006, Dijon, France.

6. TORRES, C. A., TREINT, F. e et al. Asphaltenes Pipeline Cleanout: A Horizontal Challenge for Coiled Tubing. SPE/ICoTA (Coiled Tubing Conference and Exhibition), The Woodlands, Texas (2005).

7. WANG, R.L. Smart Choice after the Accident. Oil and Gas Pipelines, Nº 2 (2010).

8. Acknowledgements

The authors acknowledge the support provided by the French Research Institute for Exploitation of the Brazilian National Agency of Petroleum, the Sea IFREMER, Natural Gas and Biofuels ANP (PRH26), the Petrobras and the Pernambuco Research Agency FACEPE (Projeto APQ-0775-1.08/10).